

Adaptive Reduced-Rank MMSE Filtering With Interpolated FIR Filters and Adaptive Interpolators

Rodrigo C. de Lamare and Raimundo Sampaio-Neto

Abstract—In this letter, we propose a broadly applicable reduced-rank filtering approach with adaptive interpolated finite impulse response (FIR) filters in which the interpolator is rendered adaptive. We describe the interpolated minimum mean squared error (MMSE) solution and propose normalized least mean squares (NLMS) and affine-projection (AP) algorithms for both the filter and the interpolator. The resulting filtering structures are considered for equalization and echo cancellation applications. Simulation results showing significant improvements are presented for different scenarios.

Index Terms—Adaptive algorithms, adaptive equalization, echo cancellation, interpolated FIR filters, reduced-rank filtering.

I. INTRODUCTION

REDUCED-RANK filtering [1], [2] and other short-data-record methods [3] are useful in low sample support situations where they can offer improved convergence performance at an affordable complexity. In this context, adaptive interpolated finite impulse response (AIFIR) filters [4], [5] represent an interesting alternative for substituting classical adaptive FIR filters. These structures retain the advantages of original interpolated FIR ones and present an error surface with a global minimum if the mean squared error (MSE) cost function is used [6]. In some applications, they show a better convergence rate and can reduce the computational burden for filtering and coefficient updating, due to the reduced number of adaptive elements. In this work, we propose a novel and effective AIFIR filter scheme in which the interpolator is also made adaptive for performing adaptive reduced-rank filtering. We describe the interpolated minimum mean squared error (MMSE) filter solution and introduce normalized least mean square (NLMS) and affine-projection (AP) algorithms for both IFIR filter and interpolator. The novel AIFIR scheme and algorithms are compared with conventional AIFIR filters with fixed interpolators, full-rank FIR filters and recent approaches such as the multistage Wiener filter (MWF) [1] and the auxiliary-vector filtering (AVF) with nonorthogonal auxiliary vectors (AVs) [3].

II. LINEAR INTERPOLATED MMSE FILTERING

Here, we describe linear interpolated filters based on the MSE criterion and detail the underlying principles of the proposed structure. Fig. 1 shows the structure of an AIFIR filter, where an

adaptive interpolator and an adaptive reduced-rank filter are employed. The $N \times 1$ observation vector $\mathbf{r}(i) = [r_0^{(i)} \dots r_{N-1}^{(i)}]^T$, where $(\cdot)^T$ is the transpose operator, is filtered by the interpolator filter $\mathbf{v}(i) = [v_0^{(i)} \dots v_{N_I-1}^{(i)}]^T$, yielding the interpolated observation vector $\mathbf{r}_I(i)$, which is projected onto an $N/L \times 1$ -dimensional vector $\bar{\mathbf{r}}_I(i)$. This procedure corresponds to removing $L - 1$ samples of $\mathbf{r}_I(i)$ of each set of L consecutive ones and then computing the inner product of $\bar{\mathbf{r}}_I(i)$ with the N/L -dimensional vector of filter coefficients $\mathbf{w}(i)$. The projected interpolated observation vector $\bar{\mathbf{r}}_I(i) = \mathbf{D}\mathbf{r}_I(i)$ is obtained with the aid of the $N/L \times N$ projection matrix \mathbf{D} that is mathematically equivalent to uniform signal decimation on the $N \times 1$ vector $\mathbf{r}_I(i)$. An interpolated MMSE filter with interpolation factor L can be designed by choosing the structure of \mathbf{D} as

$$\mathbf{D} = \begin{bmatrix} 1 & 0 & 0 & 0 & 0 & \dots & 0 & 0 & 0 & 0 & 0 \\ \vdots & \vdots & \vdots & \vdots & \vdots & \vdots & \vdots & \vdots & \vdots & \vdots & \vdots \\ \underbrace{0 \quad \dots \quad 0}_{m-1L \text{ zeros}} & & 1 & 0 & \dots & 0 & 0 & 0 & 0 & 0 & 0 \\ \vdots & \vdots & \vdots & \vdots & \vdots & \ddots & \vdots & \vdots & \vdots & \vdots & \vdots \\ \underbrace{0 \quad 0 \quad 0 \quad 0 \quad 0 \quad \dots \quad 0}_{(N/L-1)L \text{ zeros}} & & & & & & 1 & 0 & \dots & 0 & 0 \end{bmatrix} \quad (1)$$

where $m(m = 1, 2, \dots, N/L)$ denotes the m th row. The key strategy in the proposed approach, which allows us to devise solutions for both interpolator and reduced-rank filters, is to express the output $x(i) = \mathbf{w}^H(i)\bar{\mathbf{r}}_I(i)$, where $(\cdot)^H$ denotes Hermitian transpose, as a function of $\mathbf{w}(i)$ and $\mathbf{v}(i)$

$$\begin{aligned} x(i) &= w_0^* \mathbf{v}^H(i) \mathbf{r}_0^{(i)} + w_1^* \mathbf{v}^H(i) \mathbf{r}_1^{(i)} \\ &\quad + \dots + w_{N/L-1}^* \mathbf{v}^H(i) \mathbf{r}_{N/L-1}^{(i)} \\ &= \mathbf{v}^H(i) \left[\mathbf{r}_0^{(i)} \dots \mathbf{r}_{N/L-1}^{(i)} \right] \mathbf{w}^*(i) \\ &= \mathbf{v}^H(i) \mathfrak{R}(i) \mathbf{w}^*(i) \end{aligned} \quad (2)$$

where $\mathbf{u}(i) = \mathfrak{R}(i) \mathbf{w}^*(i)$, the coefficients of the IFIR filter and the interpolator weight vectors $\mathbf{w}(i)$ and $\mathbf{v}(i)$ are complex, the asterisk denotes complex conjugation, $\mathbf{r}_s(i)$ is a length N_I segment of the observation vector $\mathbf{r}(i)$ beginning at $r_{s \times L}(i)$, and

$$\mathfrak{R}(i) = \begin{bmatrix} r_0^{(i)} & r_L^{(i)} & \dots & r_{(N/L-1)L}^{(i)} \\ r_1^{(i)} & r_{L+1}^{(i)} & \dots & r_{(N/L-1)L+1}^{(i)} \\ \vdots & \vdots & \ddots & \vdots \\ r_{N_I-1}^{(i)} & r_{L+N_I}^{(i)} & \dots & r_{(N/L-1)L+N_I-1}^{(i)} \end{bmatrix}. \quad (3)$$

Manuscript received May 18, 2004; revised September 16, 2004. This work was supported by CNPq. The associate editor coordinating the review of this manuscript and approving it for publication was Prof. Dimitris A. Pados.

The authors are with CETUC/PUC-RIO, 22453-900, Rio de Janeiro, Brazil (e-mail: delamare@infolink.com.br; raimundo@cetuc.puc-rio.br).

Digital Object Identifier 10.1109/LSP.2004.842290

The MMSE expressions for both interpolator and reduced-rank filters can be computed if we consider the cost function

$$J_{MSE}(\mathbf{v}(i), \mathbf{w}(i)) = E \left[\|b(i) - \mathbf{v}^H(i) \mathfrak{R}(i) \mathbf{w}^*(i)\|^2 \right] \quad (4)$$

where $b(i)$ is the desired output, and $E[\cdot]$ denotes expected value. By fixing the interpolator filter $\mathbf{v}(i)$ and minimizing (4) with respect to $\mathbf{w}(i)$, the interpolated Wiener filter weight vector is

$$\mathbf{w}(i) = \mathbf{f}(\mathbf{v}) = \bar{\mathbf{R}}^{-1}(i) \bar{\mathbf{p}}(i) \quad (5)$$

where $\bar{\mathbf{R}}(i) = E[\bar{\mathbf{r}}_I(i) \bar{\mathbf{r}}_I^H(i)]$, $\bar{\mathbf{p}} = E[b^*(i) \bar{\mathbf{r}}_I(i)]$, $\bar{\mathbf{r}}_I(i) = \mathfrak{R}^T(i) \mathbf{v}^*(i)$, and by fixing $\mathbf{w}(i)$ and minimizing (4) with respect to $\mathbf{v}(i)$, we arrive at

$$\mathbf{v}(i) = \mathbf{g}(\mathbf{w}) = \bar{\mathbf{R}}_u^{-1}(i) \bar{\mathbf{p}}_u(i) \quad (6)$$

where $\bar{\mathbf{R}}_u(i) = E[\mathbf{u}(i) \mathbf{u}^H(i)]$, $\bar{\mathbf{p}}_u = E[b^*(i) \mathbf{u}(i)]$, and $\mathbf{u}(i) = \mathfrak{R}(i) \mathbf{w}^*(i)$. Note that (5) and (6) are not closed-form solutions for $\mathbf{w}(i)$ and $\mathbf{v}(i)$ since (5) is a function of $\mathbf{v}(i)$, and (6) depends on $\mathbf{w}(i)$, and thus, one has to iterate (5) and (6) with an initial guess to obtain a solution. The associated MSE expressions are

$$J_{MSE}(\mathbf{v}, \mathbf{f}(\mathbf{v})) = J(\mathbf{v}) = \sigma_b^2 - \bar{\mathbf{p}}^H(i) \bar{\mathbf{R}}^{-1}(i) \bar{\mathbf{p}}(i) \quad (7a)$$

$$J_{MSE}(\mathbf{g}(\mathbf{w}), \mathbf{w}) = \sigma_b^2 - \bar{\mathbf{p}}_u^H(i) \bar{\mathbf{R}}_u^{-1}(i) \bar{\mathbf{p}}_u(i) \quad (7b)$$

where $\sigma_b^2 = E[\|b(i)\|^2]$. We remark that points of global minimum of (4) can be obtained by $\mathbf{v}_{opt} = \arg \min_{\mathbf{v}} J(\mathbf{v})$ and $\mathbf{w}_{opt} = \mathbf{f}(\mathbf{v}_{opt})$ or $\mathbf{w}_{opt} = \arg \min_{\mathbf{w}} J_{MSE}(\mathbf{g}(\mathbf{w}), \mathbf{w})$ and $\mathbf{v}_{opt} = \mathbf{g}(\mathbf{w}_{opt})$. At a minimum point, (7a) equals (7b), and the MMSE for the proposed structure is achieved. We further note that since $J(\mathbf{v}) = J(t\mathbf{v})$, for every $t \neq 0$, then if \mathbf{v}^* is a point of global minimum of $J(\mathbf{v})$, then $t\mathbf{v}^*$ is also a point of global minimum. Therefore, points of global minimum (optimum interpolator filters) can be obtained by $\mathbf{v}^* = \arg \min_{\|\mathbf{v}\|=1} J(\mathbf{v})$. Since the existence of at least one point of global minimum of $J(\mathbf{v})$ for $\|\mathbf{v}\| = 1$ is guaranteed by the theorem of Weierstrass [7], then the existence of (infinite) points of global minimum is also guaranteed for the cost function in (4). For a gradient search algorithm, the cost function should not exhibit points of local minimum. Despite the fact that an analytical proof is not yet available, it is conjectured that (4) has this property. To support this claim, the plot of the error-performance surface of $J(\mathbf{v})$ [for small interpolator filter length $N_I (N_I \leq 3)$, \mathbf{v} can be expressed in spherical coordinates, and a surface can be constructed], for various scenarios, reveals that $J(\mathbf{v})$ has a global minimum value (as it should) but does not exhibit local minima, which implies that (4) has no local minima either [if the cost function in (4) had a point of local minimum, then $J(\mathbf{v})$ in (7a) should also exhibit a point of local minimum, even though the reciprocal is not necessarily true: A point of local minimum of $J(\mathbf{v})$ may correspond to a saddle point of $J_{MSE}(\mathbf{v}, \mathbf{w})$, if it exists]. In Section III, we propose an iterative solution via adaptive algorithms.

III. ADAPTIVE ALGORITHMS

We describe NLMS and AP algorithms that adjust the parameters of the interpolator and the reduced-rank filter based on the

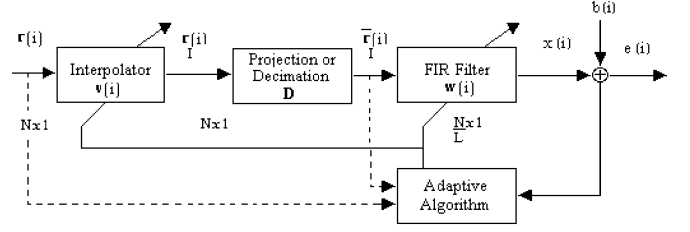


Fig. 1. Proposed adaptive reduced-rank filter structure.

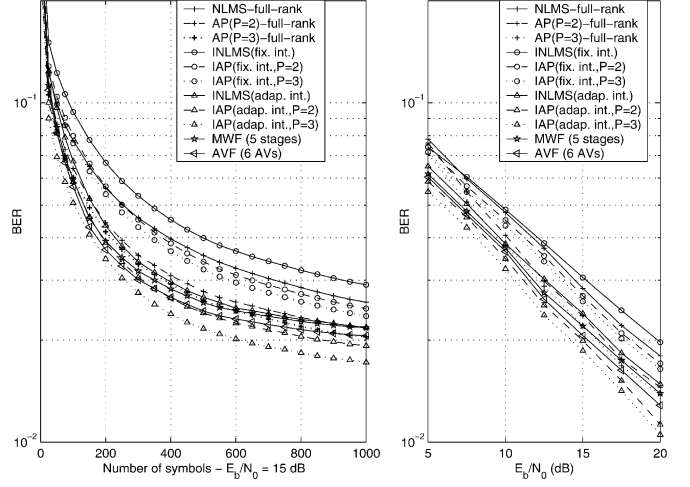


Fig. 2. BER performance of the equalizers with $N = 32$, $L = 4$, $N_{tr} = 200$, $\mathbf{v}(0) = [0.5 \ 1 \ 0.5]^T$. The optimized parameters are $\mu_0 = 0.15$ and $\eta_0 = 0.015$ for the NLMS and $\mu_0 = 0.1$ and $\eta_0 = 0.0075$ for the APs.

minimization of the MSE. The novel structure gathers fast convergence, low complexity, and additional flexibility since the designer can adjust the interpolation factor L and the length of the interpolator N_I , depending on the need for fast convergence and response to changing environments. In addition, the proposed scheme trades off one adaptive algorithm with full rank in favor of two reduced-rank recursions, which are operating in parallel.

A. Interpolated NLMS (INLMS) Algorithm

Consider the following unconstrained cost function:

$$J = \|\mathbf{w}(i+1) - \mathbf{w}(i)\|^2 + \|\mathbf{v}(i+1) - \mathbf{v}(i)\|^2 + \text{Re} [\lambda_1^* (b(i) - \mathbf{w}^H(i+1) \bar{\mathbf{r}}_I(i))] + \text{Re} [\lambda_2^* (b(i) - \mathbf{v}^H(i+1) \mathbf{u}(i))] \quad (8)$$

where λ_1 and λ_2 are scalar Lagrange multipliers, the operator $\text{Re}(\cdot)$ selects the real part of the argument, and $\mathbf{u}(i) = \mathfrak{R}(i) \mathbf{w}^*(i)$. Taking the gradient terms of (8) with respect to $\mathbf{w}(i+1)$, $\mathbf{v}(i+1)$, λ_1 , and λ_2 , setting the gradient terms to zero and solving the resulting equations above yields

$$e(i) = b(i) - \mathbf{w}(i)^H \bar{\mathbf{r}}_I(i) \quad (9)$$

$$\mathbf{v}(i+1) = \mathbf{v}(i) + \eta(i) e^*(i) \mathbf{u}(i) \quad (10)$$

$$\mathbf{w}(i+1) = \mathbf{w}(i) + \mu(i) e^*(i) \bar{\mathbf{r}}_I(i) \quad (11)$$

where $\mu(i) = (\mu_0 / \|\bar{\mathbf{r}}_I(i)\|^2)$ and $\eta(i) = (\eta_0 / \|\mathbf{u}(i)\|^2)$ are the step sizes of the algorithm, and μ_0 and η_0 are the convergence factors. The new method has a computational complexity $O(N/L + N_I)$.

B. Interpolated Affine Projection (IAP) Algorithm

The AP algorithm is one of the prominent adaptive algorithms that can achieve a good compromise between fast convergence and low computational complexity. By adjusting the number of projections, the performance of the algorithm can be controlled from that of the NLMS to that of the RLS algorithm [6]. The AP updates its coefficient vector such that the new solution belongs to the intersection of P hyperplanes defined by the present and the $P - 1$ previous data pairs. The observation matrix is $\mathbf{Y}(i) = [\bar{\mathbf{r}}_I(i) \dots \bar{\mathbf{r}}_I(i - P + 1)]$, $\mathbf{u}(i) = \Re(i)\mathbf{w}^*(i)$, $\mathbf{U}(i) = [\mathbf{u}(i) \dots \mathbf{u}(i - P + 1)]$, the desired output vector $\mathbf{b}(i) = [b(i) \dots b(i - P + 1)]^T$ in this case comprises P outputs, and the error vector is given by

$$\mathbf{e}(i) = \mathbf{b}^*(i) - \mathbf{Y}^H(i)\mathbf{w}(i) = \mathbf{b}^*(i) - \mathbf{U}^H(i)\mathbf{v}(i). \quad (12)$$

Consider the following Lagrangian cost function:

$$\begin{aligned} J = & \|\mathbf{w}(i+1) - \mathbf{w}(i)\|^2 + \|\mathbf{v}(i+1) - \mathbf{v}(i)\|^2 \\ & + \text{Re} \left[(\mathbf{b}(i) - \mathbf{Y}^H(i)\mathbf{w}(i+1))^H \boldsymbol{\lambda}_1 \right] \\ & + \text{Re} \left[(\mathbf{b}(i) - \mathbf{U}^H(i)\mathbf{v}(i+1))^H \boldsymbol{\lambda}_2 \right] \end{aligned} \quad (13)$$

where $\boldsymbol{\lambda}_1$ and $\boldsymbol{\lambda}_2$ are vectors of Lagrange multipliers. By calculating the gradient terms of (13), setting them to zero, and solving the resulting equations, we arrive at the following algorithm:

$$\mathbf{t}(i) = (\mathbf{Y}^H(i)\mathbf{Y}(i) + \delta\mathbf{I})^{-1}\mathbf{e}(i) \quad (14)$$

$$\mathbf{t}_v(i) = (\mathbf{U}^H(i)\mathbf{U}(i) + \delta\mathbf{I})^{-1}\mathbf{e}(i) \quad (15)$$

$$\mathbf{v}(i+1) = \mathbf{v}(i) + \eta_0\mathbf{U}(i)\mathbf{t}_v(i) \quad (16)$$

$$\mathbf{w}(i+1) = \mathbf{w}(i) + \mu_0\mathbf{Y}(i)\mathbf{t}(i) \quad (17)$$

where μ_0 and η_0 are the convergence factors, and δ is a small constant used to improve robustness. The IAP algorithm described here has a computational complexity $O(P \times N/L + P \times N_I + 2K_{\text{inv}}P^2)$, where K_{inv} is the number of operations required to invert a $P \times P$ matrix.

IV. SIMULATIONS

In this section, the filtering structures and algorithms described in Sections II and III are used for equalization and echo cancellation purposes and compared with the full rank, the AIFIR with fixed interpolators, the MWF [1], and the AVF of [3]. The convergence and bit error rate (BER) performance of the resulting equalizers are assessed in a binary phase-shift keying (BPSK) [8], [9] system for a range of settings. After coherent demodulation, matched filtering, and sampling at data rate $1/T_b$, the received signal vector is $\mathbf{r}(i) = \mathbf{s}(i) + \mathbf{n}(i)$, where $\mathbf{s}(i) = [s(i) \dots s(i - N + 1)]^T$, $s(i) = \sum_{l=0}^{L_p-1} h_l(i)b(i-l)$, the channel coefficients at time i are $h_0(i) \dots h_{L_p-1}(i)$, the complex symbol $b(i) \in \{\pm 1 + j0\}$, L_p is the channel length, and $\mathbf{n}(i) = [n(i) \dots n(i - N + 1)]^T$ is a complex white Gaussian noise vector with covariance matrix $\sigma_n^2\mathbf{I}$. The detected symbols are given by $\hat{b}(i) = \text{sgn}(\text{Re}(\mathbf{w}^H(i)\bar{\mathbf{r}}_I(i)))$, and the SNR is defined by $\text{SNR} = E_b/N_0 = \sigma_b^2/\sigma_n^2$. We consider both stationary and typical mobile channel models. The mobile channel coefficients for the users are $h_l(i) = p_l\alpha_l(i)$, where $\alpha_l(i) (l = 0, 1, \dots, L_p - 1)$ is obtained with Clarke's model

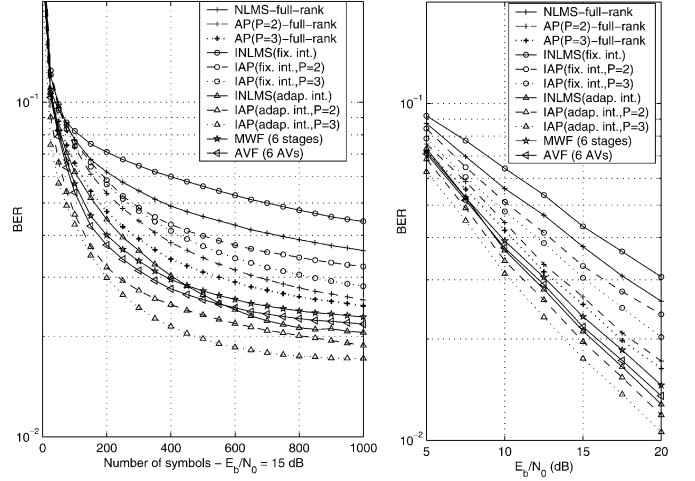


Fig. 3. BER performance of the equalizers with $N = 32$, $L = 4$, $N_{tr} = 200$, $f_d T_b = 0.005$, $\mathbf{v}(0) = [0.5 \ 1 \ 0.5]^T$. The optimized parameters are $\mu_0 = 0.075$ and $\eta_0 = 0.005$ for the NLMS, whereas $\mu_0 = 0.05$ and $\eta_0 = 0.005$ for the APs.

[8]. The results are shown in terms of the normalized Doppler frequency $f_d T_b$ (cycles/symbol). For the stationary channel, which is found in [9] and exhibits deep spectral nulls, we make $h_l(i) = p_l$ and use the coefficients $p_0 = 0.227$, $p_1 = 0.460$, $p_2 = 0.688$, $p_3 = 0.460$, and $p_4 = 0.227$. We compare the full-rank and the reduced-rank equalizers with the NLMS and AP algorithms for both fixed and adaptive interpolators, as depicted in the legends of Figs. 2 and 3. The algorithms use N_{tr} training symbols and then switch to decision-directed mode. The convergence factors of the algorithms, the number of stages of the MWF, and AVs of the AVF have been optimized. Simulations are averaged over 100 runs and 1000 symbols.

We have conducted experiments in order to obtain the most adequate dimension for the interpolator $\mathbf{v}(i)$, with values ranging from $N_I = 3$ to $N_I = 6$. The results indicated that BER performance was not sensitive to an increase in the number of taps in $\mathbf{v}(i)$. Thus, for this reason and to keep the complexity low, we selected $N_I = 3$. In Fig. 2, we show the results for the stationary channel scenario. In Fig. 3, the results are depicted for a four-path time-varying fading mobile channel, where each path is spaced by four symbols, with the profile given by $p_0 = 0.741$, $p_4 = 0.370$, $p_8 = 0.222$, and $p_{12} = 0.074$.

The reduced-rank receivers that employ adaptive interpolators achieve a superior convergence and BER performance to full-rank (that need long transmissions to outperform our scheme) and reduced-rank equalizers that do not update their interpolators. The improvements are even more significant for the time-varying channel, as shown in Fig. 3. The AP algorithms perform better than NLMS recursions, and as the number of projections P is increased, so is the performance. The novel AIFIR approach using the NLMS is comparable to the MWF and the AVF and is superior to the MWF and the AVF when using the AP, whereas its complexity is inferior to the AVF and the MWF. A disadvantage of the AIFIR as compared to the MWF and the AVF is an extra effort to tune the convergence factors.

In echo cancellation applications, the objective of adaptive filtering is to estimate the acoustic echo path $b(i)$ to be cancelled. Here, we consider an echo path measured in a car, as shown in

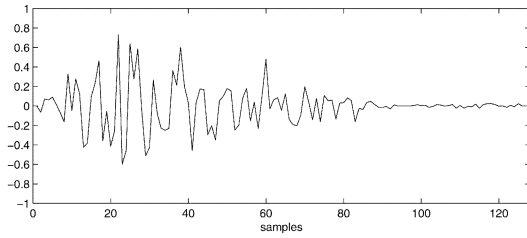


Fig. 4. Car echo path.

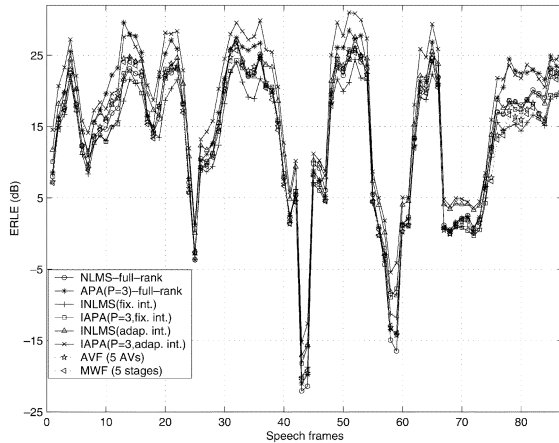


Fig. 5. Segmental ERLE curves with $N = 128$, $L = 2$, and $\mathbf{v}(0) = [0.5 \ 1 \ 0.5]^T$. The optimized parameters are $\mu_0 = 0.15$ and $\eta_0 = 0.00025$ for the NLMS, while $\mu_0 = 0.15$ and $\eta_0 = 0.00025$ for the APs.

Fig. 4, and use real speech and echo signals that are sampled at 8 KHz and quantized to 16 bits. To measure the effectiveness of the proposed scheme, we have computed the *echo return loss enhancement* (ERLE), given by $ERLE = 10 \log_{10} \frac{E[b^2(i)]}{E[e^2(i)]}$ dB, where $e(i)$ is the error signal [10]. To obtain the most adequate dimension for the interpolator $\mathbf{v}(i)$, we carried out experiments with values ranging from $N_I = 3$ to $N_I = 6$ and measured the ERLE performance. The results reveal that $N_I = 3$ achieves a satisfactory performance at a reduced complexity.

We show the results in terms of segmental ERLE, whose estimates are obtained by averaging $b^2(i)$ and $e^2(i)$ over 20 ms frames (160 samples). The curves for the echo cancellation experiments, depicted in Figs. 5 and 6, indicate that the reduced-rank structures that employ adaptive interpolators have a better performance than the full-rank echo canceller for $L = 2$. For $L = 4$, the proposed scheme achieves a comparable performance to the full-rank filter with only 35 ($N/L + N_I$) adaptive elements. The echo cancellers with adaptive interpolators are significantly superior to the fixed interpolated version in all situations. In comparison with the MWF and the AVF, the novel AIFIR approach is slightly superior with the NLMS and considerably better with the AP.

The simulations results reveal that the algorithms always converge to the same minimum value, provided that adequate step sizes are chosen, $\mathbf{v}(0) \neq \mathbf{0}$ (this eliminates the signal before decimation) and independently of any initialization, which is an important feature that advocates the nonexistence of local minima. A convergence analysis of the proposed method considers the trajectory of both parameter vectors in order to obtain the mean tap weight vectors,

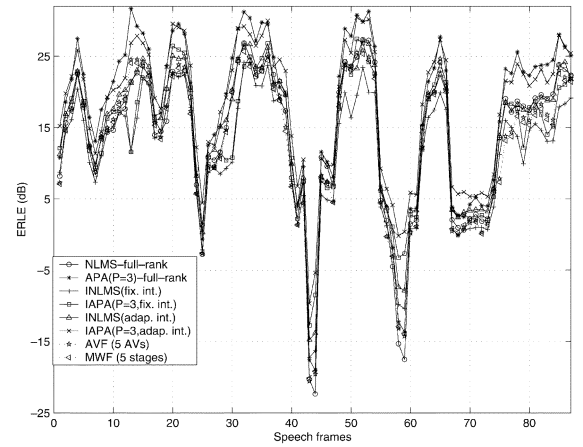


Fig. 6. Segmental ERLE curves with $N = 128$, $L = 4$, and $\mathbf{v}(0) = [0.5 \ 1 \ 0.5]^T$. The optimized parameters are $\mu_0 = 0.15$ and $\eta_0 = 0.00025$ for the NLMS, whereas $\mu_0 = 0.15$ and $\eta_0 = 0.00025$ for the APs.

that is, $\boldsymbol{\epsilon}_w = \mathbf{w} - \mathbf{w}_{opt}$ and $\boldsymbol{\epsilon}_v = \mathbf{v} - \mathbf{v}_{opt}$ and the excess MSE. For instance, the mean tap vector analysis yields $E[\boldsymbol{\epsilon}_w^T(i+1)\boldsymbol{\epsilon}_v^T(i+1)]^T = \mathbf{A}(i)E[\boldsymbol{\epsilon}_w^T(i)\boldsymbol{\epsilon}_v^T(i)]^T + \mathbf{B}(i)$, where $\mathbf{A}(i)$ and $\mathbf{B}(i)$ are functions of $\mathbf{w}(i)$, $\mathbf{v}(i)$, and $\mathbf{r}(i)$. For stability, the convergence factors should be chosen so that the eigenvalues of $\mathbf{A}^H(i)\mathbf{A}(i)$ are less than one. A complete convergence analysis of the new scheme, conditions, and proofs are not included here due to lack of space and are intended for a future and longer paper.

V. CONCLUSIONS

We proposed low-complexity reduced-rank filters based on AIFIR filters with adaptive interpolators and developed NLMS and AP adaptive algorithms for the proposed schemes. These structures were tested for equalization and echo cancellation, showing superior performance to previously reported AIFIR techniques with fixed interpolators, full-rank filters, and the MWF and AVF methods.

REFERENCES

- [1] J. S. Goldstein, I. S. Reed, and E. L. L. Scharf, "A multistage representation of the Wiener filter based on orthogonal projections," *IEEE Trans. Inf. Theory*, vol. 44, no. 7, pp. 2943–2959, Nov. 1998.
- [2] D. A. Pados and S. N. Batalama, "Joint space-time auxiliary-vector filtering for DS/CDMA systems with antenna arrays," *IEEE Trans. Commun.*, vol. 47, no. 9, pp. 1406–1415, Sep. 1999.
- [3] G. N. Karystinos, H. Qian, M. J. Medley, and S. N. Batalama, "Short-data-record adaptive filtering: The auxiliary-vector algorithm," *Digit. Signal Process., Special Issue Defense Appl.*, vol. 12, pp. 193–222, Jul. 2002.
- [4] A. Abousaada, T. Abousnasr, and W. Steenaert, "An echo tail canceller based on adaptive interpolated FIR filtering," *IEEE Trans. Circuits Syst. II, Analog. Digit. Signal Process.*, vol. 39, no. 7, pp. 409–416, Jul. 1992.
- [5] L. S. Resende, C. A. F. Rocha, and M. G. Bellanger, "A linearly constrained approach to the interpolated FIR filtering problem," in *Proc. IEEE Int. Conf. Acoust. Speech Signal Process.*, 2000.
- [6] S. Haykin, *Adaptive Filter Theory*, 4th ed. Englewood Cliffs, NJ: Prentice-Hall, 2002.
- [7] D. P. Bertsekas, *Nonlinear Programming*, 2nd ed. Nashua, NH: Athena Scientific, 1999.
- [8] T. S. Rappaport, *Wireless Communications*. Englewood Cliffs, NJ: Prentice-Hall, 1996.
- [9] J. G. Proakis, *Digital Communications*, 3rd ed. New York: McGraw-Hill, 1995.
- [10] A. Gilloire, E. Moulines, D. Slock, and P. Duhamel, "State of the art in acoustic echo cancellation," in *Digital Signal Processing in Telecommunications*. London, U.K.: Springer-Verlag, 1996, pp. 45–92.